

pubs.acs.org/NanoLett Letter

Nanoparticle-Enhanced RT-QuIC (Nano-QuIC) Diagnostic Assay for Misfolded Proteins

Peter R. Christenson, Manci Li, Gage Rowden, Peter A. Larsen,* and Sang-Hyun Oh*



Cite This: Nano Lett. 2023, 23, 4074-4081



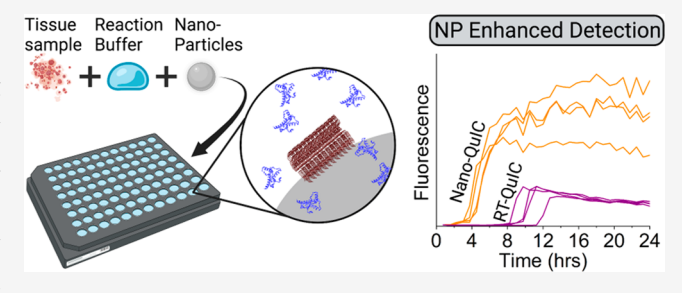
ACCESS I

III Metrics & More

Article Recommendations

s Supporting Information

ABSTRACT: Misfolded proteins associated with various neuro-degenerative diseases often accumulate in tissues or circulate in biological fluids years before the clinical onset, thus representing ideal diagnostic targets. Real-time quaking-induced conversion (RT-QuIC), a protein-based seeded-amplification assay, holds great potential for early disease detection, yet challenges remain for routine diagnostic application. Chronic Wasting Disease (CWD), associated with misfolded prion proteins of cervids, serves as an ideal model for evaluating new RT-QuIC methodologies. In this study, we investigate the previously untested hypothesis that



incorporating nanoparticles into RT-QuIC assays can enhance their speed and sensitivity when applied to biological samples. We show that adding 50 nm silica nanoparticles to RT-QuIC experiments (termed Nano-QuIC) for CWD diagnostics greatly improves the performance by reducing detection times 2.5-fold and increasing sensitivity 10-fold by overcoming the effect of inhibitors in complex tissue samples. Crucially, no false positives were observed with these 50 nm silica nanoparticles, demonstrating the enhanced reliability and potential for diagnostic application of Nano-QuIC in detecting misfolded proteins.

KEYWORDS: amyloid, prions, RT-QuIC, protein misfolding, gold nanoparticle, silica nanoparticle

athological amyloids formed by misfolded proteins (MPs) are found in many human and animal neurodegenerative diseases, including Alzheimer's Disease (misfolded A β and tau), Parkinson's disease (misfolded α -synuclein), and prion diseases (misfolded cellular prion proteins, PrPC). 1-4 Amyloid formation originates via the misfolding of functional proteins into insoluble and degradation-resistant amyloid fibrils that are rich in β -sheet structures. A notable feature across the spectrum of neurodegenerative disease is that the production and deposition of affiliated MPs typically begin years before the onset of clinical symptoms. Consequently, developing highly sensitive diagnostic methods for detecting MPs during presymptomatic stages of neurodegenerative diseases is a critical research area. 5-8 If successful, such methods could facilitate the strategic enrollment of patients in clinical trials and the deployment of therapeutic interventions during the earliest stages of neurodegenerative disease.

Current diagnostics for MP diseases are limited. 9,10 Conventional assays rely heavily on antibody-based enzyme-linked immunosorbent assays (ELISA) and immunohistochemistry (IHC) technologies, which are expensive and time-consuming and require substantial training and expertise to operate. Additionally, antibodies used in these assays often fail to differentiate between native and misfolded proteins due to poor specificity, necessitating protein digestion to enrich MPs. This approach can affect diagnostic sensitivity through the destruction of particular MP-associated strains. 11 Together, these antibody-based assays are limited in the identification of

early stage MPs and are primarily used on tissues collected post-mortem. Real-time quaking-induced conversion (RT-QuIC) has emerged as one of the most promising assays for early diagnosis of various MP-related neurodegenerative diseases. 5,6,9,12,13 Briefly, in RT-QuIC, small volumes of biological samples (e.g., lymph nodes, cerebral spinal fluid, skin, etc.) are seeded into a solution containing an excess of recombinant protein substrate (e.g., recombinant hamster prion protein [rHaPrP]) that, in the presence of a specific MP template, begins to misfold and form amyloids after a period of shaking and incubation. A fluorescent dye Thioflavin T (ThT) then binds to the misfolded substrate protein, yielding a detectable signal based on the basis of light excitation. If MPs are absent in the original biological seed, then misfolding of the substrate protein does not occur, allowing for a clear distinction between the presence or absence of MP-induced amyloid. Amyloid formation in RT-QuIC generally follows sigmoidal kinetics partitioned into three distinct phasesnucleation, growth, and stationary phases-corresponding to particular molecular mechanisms that dominate the RT-QuIC

Received: March 15, 2023 Revised: April 22, 2023 Published: April 26, 2023





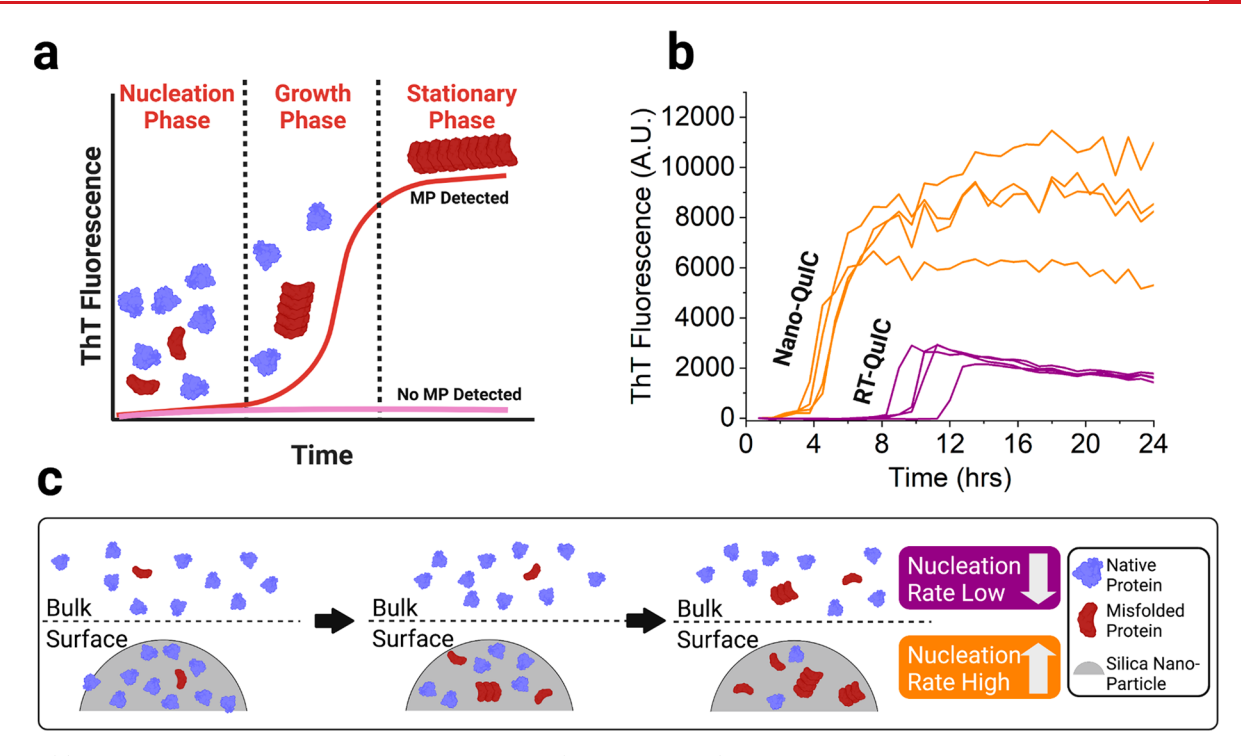


Figure 1. (a) Summary of fibril growth under normal conditions (no nanoparticles) showing nucleation, growth, and stationary phases. Sigmoidal curve represents MP detection, and flat line represents no MP detection. (b) Results from Nano-QuIC and traditional RT-QuIC. (Nano-QuIC conditions: 48 °C, 2.5 mg/mL 50 nm silica NPs). (c) Schematic of the Nano-QuIC seeded-amplification mechanism. In Nano-QuIC, silica NPs promote primary nucleation at a higher rate than bulk solution methods such as RT-QuIC.

reaction (Figure 1A). While RT-QuIC has been successfully applied to detect several MPs associated with a variety of neurodegenerative diseases (e.g., TDP-43, Tau, Alphasynuclein, infectious prions, etc.)^{6,13} the complexity of biological samples still poses challenges for clinical diagnostic applications. For example, the assay has low kinetic efficiency, often taking up to 48 h to complete a standard test. Additionally, although it is more sensitive than conventional protein detection methods (i.e., ELISA and immunohistochemistry),14 natural inhibitors present within biological samples can interfere with reaction kinetics, producing falsenegative results.^{7,12,15,16} To harness RT-QuIC's potential for early neurodegenerative diseases diagnosis, it is imperative to develop novel methodologies that enhance assay performance, especially diagnostic sensitivity, and facilitate the transition of RT-QuIC from basic research to clinical application.

Chronic wasting disease (CWD), a prion disease affecting cervids across North America, Scandinavia, and South Korea, ^{17–20} involves the misfolding of cellular prion protein (PrP^C) into amyloid fibrils by CWD prions (PrP^{CWD}), similar to the protein misfolding processes observed across the neurodegenerative disease spectrum. Due to growing concerns about potential interspecies transmission ^{13,21} PrP^{CWD} is one of the most extensively studied MP diseases using RT-QuIC, with several protocols developed to improve assay performance for PrP^{CWD} detection. ^{7,9,13,15,22} Additionally, samples of CWD from animals are more easily obtained than samples from humans. Therefore, PrP^{CWD} serves as an ideal model MP for exploring and evaluating novel RT-QuIC methodologies.

Nanoparticles (NPs) have been used to advance diagnostics in a variety of fields^{4,23-28} and have been studied extensively for their roles in protein misfolding.²⁹⁻³⁷ When proteins adsorb onto a nanoparticle's surface, the local concentration of

the substrate increases, and protein conformation can be altered.^{35–38} This can lead to the promotion of nucleation events, which shortens the nucleation phase (Figures 1A, B). While the effects of NPs on the kinetics of amyloid formation have been characterized for several proteins,^{29–36} NPs have not been used in RT-QuIC protocols for the detection of MPs in complex biological samples.

In the present study, we applied silica NPs (siNPs) as reagents in RT-QuIC reactions to enhance the detection of CWD prions in lymphoid tissues of wild white-tailed deer. We selected nanoparticles with diameters below 100 nm, as previous research has demonstrated their potential to increase aggregation for various proteins. SiNPs were chosen as the primary focus because they are negatively charged and thus readily interact with the positively charged rHaPrP substrate. Moreover, siNPs are more cost-effective than other NP options, such as gold nanoparticles, thus leading to a more practical application. However, we also explored the performance of gold NPs to demonstrate the versatility and broad applicability of various nanoparticle types in enhancing the RT-QuIC detection of misfolded proteins in biological samples.

We observed that the RT-QuIC performance was significantly improved in the presence of siNPs, corresponding to siNP size. By exploring various combinations of NP diameters, concentrations, and reaction temperatures, we identified optimal RT-QuIC conditions represented by the highest rate of amyloid formation (RAF, see methods, Figure 1B) and the lowest false-positivity rate. We found that the addition of 50 nm siNPs optimized the RT-QuIC performance by significantly increasing both the rate of amyloid formation and ThT fluorescence (Figure 1B). Using sigmoidal-like curves, we fit the kinetic fluorescent data and extracted key parameters that describe the lag time of the nucleation phase and the time

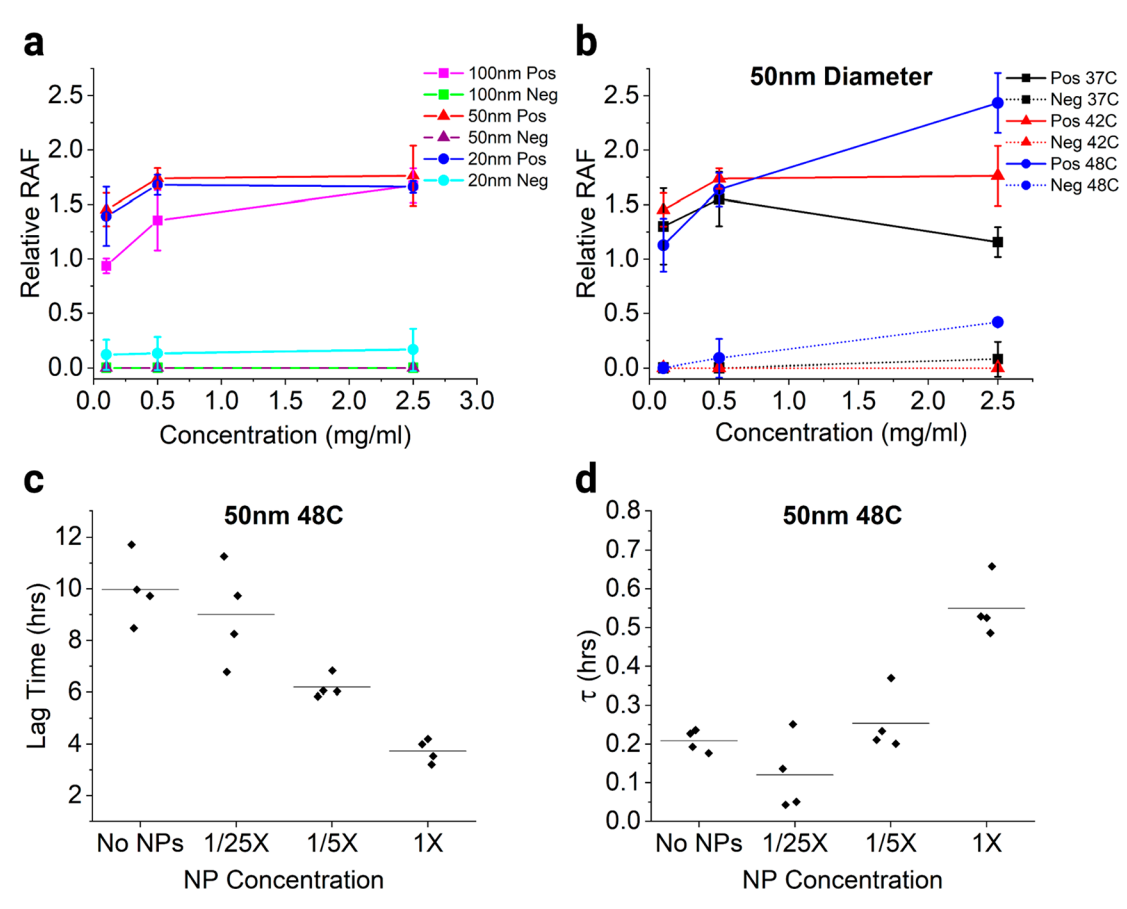


Figure 2. (a) Relative rate of amyloid formation (RAF) of various diameter and concentrations of silica NP solutions amplified at 42 $^{\circ}$ C seeded with CWD positive or negative tissue homogenates. (b) Relative RAF of solutions seeded with CWD positive or negative tissue with various concentrations of 50 nm silica NPs amplified at different temperatures. (c) The lag time of the nucleation phase vs concentration of 50 nm silica NPs at 48 $^{\circ}$ C. (d) The time constant of fibril growth (τ) vs concentration of 50 nm silica NPs at 48 $^{\circ}$ C. Unless noted otherwise, error bars show standard deviation.

constant of the growth phase. Our findings reveal that much of the speed increase is likely due to a higher nucleation rate of MP on the siNP surface compared to the bulk solution (Figure 1C). Furthermore, we demonstrated that the accelerating effects of NPs are not just limited to siNPs but can also occur by incorporating gold nanoparticles (AuNPs) in the RT-QuIC reaction. To test whether RT-QuIC with siNPs could overcome effects of inhibitors, we serially diluted CWD-positive lymphoid tissues and found that siNP-enhanced RT-QuIC can readily detect the presence of CWD prions at a concentration previously unattainable. Collectively, our results strongly indicate that the nanoparticle-enhanced RT-QuIC reaction, termed Nano-QuIC, vastly improves diagnostic performance.

RESULTS

Effects of siNP Diameter and Concentration on RT-QuIC Performance. To examine the effects of nanoparticles on RT-QuIC performance, siNPs with diameters ranging from 20 to 100 nm were added as a reagent to RT-QuIC reactions seeded with CWD positive or negative tissue homogenates (parotid lymph nodes). Concentrations of siNPs were set at 0.1 0.5, and 2.5 mg/mL. Reactions were run for 48 h at 42 °C. All diameters of siNPs examined herein affected the rate of amyloid formation (RAF, see the Supporting Methods) when compared to the RAF of reactions having no siNPs (Figure 2a). The ratio between the RAF of reactions with and without

siNPs gives a parameter known as the relative RAF. For all siNP diameters, the relative RAF increased as the concentration of the siNPs increased (Figure 2a). This led to an average time to CWD detection of 6.3 h (95% confidence interval [CI]: \pm 0.96 h) for 50 nm siNPs at 42 °C, 4.9 h faster than traditional RT-QuIC reactions of the same sample (average time to detection of 11.2 h (95% CI: \pm 1.00 h)). Importantly, the optimal siNP reaction parameters for diagnostic assessment of PrP^{CWD} positive tissues examined herein (50 nm siNPs at 42 °C) yielded no false positives.

Temperature Effects on Nano-QuIC Sensitivity and Specificity. The temperature of RT-QuIC experiments directly influences their sensitivity and specificity.³⁹ Higher temperatures typically yield higher RAFs, however, such conditions increase the risk of spontaneous misfolding of the substrate protein. Lower temperatures give lower RAF values, extending diagnostic time and potentially leading to falsenegative results but decreasing false-positivity rates. To identify optimal conditions that maximize Nano-QuIC sensitivity and specificity, experiments were performed at 37 °C, 42 °C, and 48 °C for 20–100 nm siNPs with concentrations ranging from 0.1-2.5 mg/mL (Figure 2b and Figure S1). Once again, the relative RAF was found by comparing reactions with and without siNPs. For reactions at 37 °C, all diameters of siNPs led to higher relative RAFs of CWD-positive samples vs the same samples tested with traditional RT-QuIC (Figure 2b and Figure S1). However, compared with siNP experiments

Nano Letters pubs.acs.org/NanoLett Letter

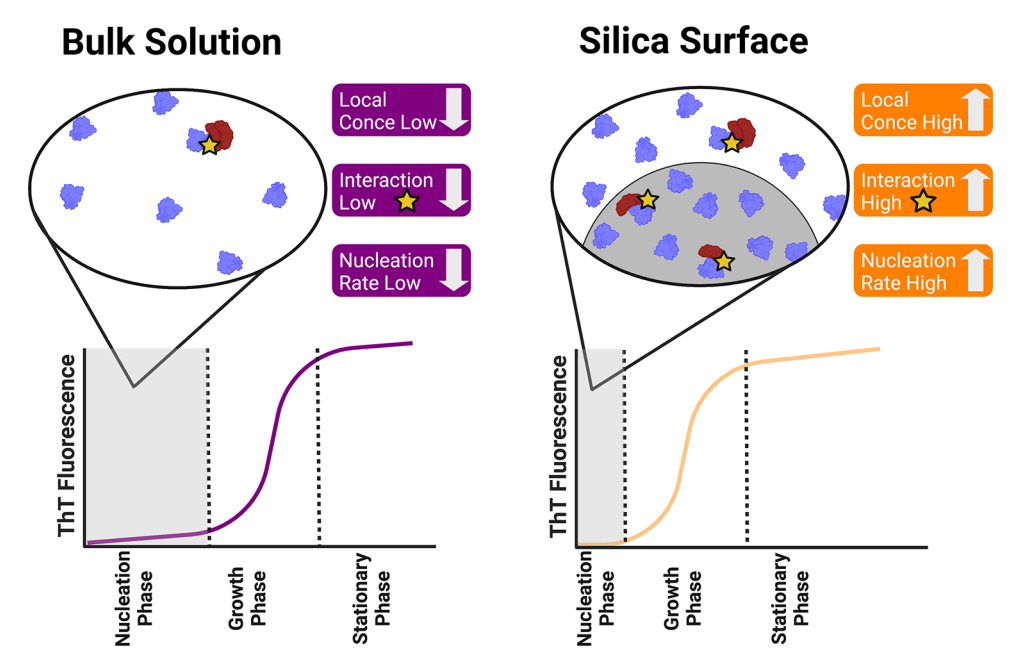


Figure 3. Schematic illustration of the proposed mechanism of action. In the bulk solution, RT-QuIC substrate is not concentrated and the number of interactions between misfolded protein and substrate is low. In proximity to the silica surface (Nano-QuIC), the local concentration of substrate is increased, partly due to electrostatic attraction and thus the interactions between misfolded protein and substrates are increased.

performed at higher temperatures, CWD-positive reactions performed at 37 °C exhibited slower RAFs. For Nano-QuIC experiments performed at 48 °C, all diameters of siNPs again led to a higher relative RAF (Figure 2b and Figure S1). Additionally, experiments performed at 48 °C had shorter detection times (higher raw RAFs) compared with reactions at lower temperatures. Nano-QuIC performed using 50 nm siNPs at 2.5 mg/mL and a temperature of 48 °C gave the largest relative RAF and the fastest detection time, just 4.1 h (95% CI: \pm 0.45 h) compared to 10.1 h (95% CI: \pm 1.44 h) for traditional RT-QuIC, a 2.5× improvement (Figure 2b). No false positive replicates were observed across our CWDnegative samples (Discussion). Using these parameters, Nano-QuIC was performed on a blinded set of 10 CWD positive and 10 CWD negative wild white-tailed deer retropharyngeal lymph nodes, and all tissues were classified with 100% sensitivity and specificity (Table S1).

Characterization of Aggregation Kinetics and Mechanism in Nano-QuIC. The formation of fibrils is a process in which misfolded proteins interact with one another to form large linear structures. Modeling fibril formation in RT-QuIC is achieved using three phases: nucleation (lag), growth (elongation), and stationary ^{37,40,41} (Figure 1a). The nucleation phase involves native proteins misfolding into nuclei units with low fluorescence values because ThT fluoresces when bound to fibrils⁴² and not to single monomers. In the elongation phase, nuclei act as templates to efficiently misfold other native proteins, ultimately producing linear fibrils. In the presence of mechanical shaking or sonication, these fibrils can break, thus creating additional nuclei for native proteins to misfold and making more fibrils. The elongation phase is characterized by exponential growth of fibrils as documented by exponential growth of ThT fluorescence (Figures 1a and 2b). In the final phase, the stationary phase, ThT fluorescence ceases to increase exponentially and stabilizes. This model accounts for both the propagation of infectious prions observed in transmissible spongiform encephalopathies (e.g., CWD or

Creutzfeldt-Jakob disease) as well as the misfolding and spread of proteins associated with various neurodegenerative diseases (e.g., Parkinson's, ALS, and Alzheimer's disease). 30-32,40,41,43

The three phases of protein amplification using RT-QuIC are modeled using sigmoidal-like curves. 40,41

$$Y = y_{i} + m_{i}x + \frac{y_{f} + m_{f}x}{1 + e^{-[(x - x_{0})/\tau]}}$$
(1)

where y_i and m_i are associated with the initial ThT fluorescence and slope of the nucleation phase. y_f and m_f are associated with the final ThT fluorescence and the slope of the stationary phase. The time to 50% of the maximum ThT fluorescence is x_o and τ is the time constant for fibril growth. The length of the nucleation phase, which is approximately the time to detection, is given by the lag time, $x_o - 2\tau$.

To characterize the kinetics of how siNPs influence RT-QuIC reactions (50 nm siNPs at 48 °C), eq 1 was used to develop fits that yielded semiquantitative values of lag time and the time constant for fibril growth (τ) for all concentrations (Supporting Methods). We observed a decrease in lag time with increasing siNP concentration (Figure 2c), indicating their crucial role in initial nuclei formation for fibrillation.⁴³

At pH 7.4, the RT-QuIC substrate rHaPrP is positively charged, whereas siNPs are negatively charged, leading to an attractive force. This likely promotes the adsorption of rHaPrP onto siNP surfaces, increasing the local effective concentration of the QuIC substrate (Figure 3). Additionally, infectious prions can adsorb onto glass and silica surfaces. Adsorbed proteins can diffuse across the surface and interact with one another. Because the local concentration of proteins on the siNP surface is higher than in the bulk reaction space, there is more opportunity for RT-QuIC substrate to interact with misfolded protein seeds, thus influencing reaction kinetics by facilitating a more efficient nucleation phase. Additionally, proteins adsorbed onto surfaces often change their conformation. These changes could make rHaPrP more susceptible to misfolding in the presence of prion

Nano Letters pubs.acs.org/NanoLett Letter

seeds, thus increasing the nucleation rate. It should be noted that the three characteristic phases of protein amplification discussed above were entirely absent from the negative samples.

The time constant for fibril growth (τ) is used to compare fibril growth phases between different RT-QuIC reaction conditions. For 50 nm siNPs at 48 °C, we observed that a higher nanoparticle concentration resulted in longer τ (Figure 2d). Additionally, the maximum ThT fluorescence of solutions with NPs was larger than solutions without NPs (Figure 1b). This observation could be accounted for if the siNPs, in the presence of mechanical shaking, are more efficiently breaking the fibrils into smaller units.³⁷ A greater number of fibril nuclei will recruit more haPrP substrate, thus contributing to an exponential growth phase. Such a mechanism would explain the unique sigmoidal curves observed in Nano-QuIC.

Nano-QuIC with Gold Nanoparticles. To demonstrate that acceleration effects of NPs on RT-QuIC performance can apply to other NP types, additional experiments were conducted using AuNPs. Fifteen nanometer citrate-capped AuNPs were added as reagents to RT-QuIC reactions to obtain final concentrations of 20.75 62.5, or 187.5 ug/mL AuNPs. CWD-positive or CWD-negative tissue homogenates were added to the solutions and RT-QuIC reactions ran for 48 h at 42 °C. RAFs were higher for all solutions containing AuNPs compared to RAFs of reactions without AuNPs (Figure 4). The fastest average time to detection was found to be 8.2 h (95% CI: ± 1.21 h) compared to the average time of detection of the no AuNP solutions: 12.5 h (95% CI: ± 1.26 h).

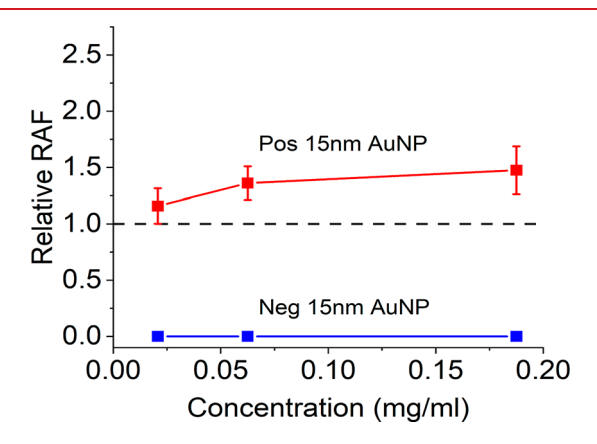


Figure 4. Relative RAF (ratio of the RAF of reactions with 15 nm AuNPs compared to those without). Assay was run at 42 $^{\circ}$ C. Error bars show standard deviation.

Enhancing Sensitivity and Overcoming Inhibitors with Nano-QuIC. Tissue dilution series experiments were performed for 50 nm siNPs at 42 °C to compare the sensitivity of Nano-QuIC and traditional RT-QuIC. 10-fold dilutions of CWD-positive tissue seeds were created from 10⁻¹ to 10⁻⁹. Subsamples of these dilutions (i.e., seeds) were then added to both the Nano-QuIC and traditional RT-QuIC reactions. Nano-QuIC and traditional RT-QuIC detected seeding activity in reactions with seeds diluted to 10⁻⁹ and 10⁻⁸, respectively, documenting the diagnostic sensitivity of these assays. However, for less dilute seeds, Nano-QuIC greatly outperformed traditional RT-QuIC. At dilutions of 10⁻¹ PrP^{CWD} positive tissue, traditional RT-QuIC exhibited no seeding activity, whereas Nano-QuIC clearly detected the presence of

PrP^{CWD} as reflected by high RAF values (Figure 5a, b). Moreover, for PrP^{CWD} positive tissue dilutions of 10⁻², Nano-QuIC yielded double the RAF yield compared to traditional RT-QuIC (Figure 5a).

Biological samples, especially from clinical settings, are extremely complex, thus making diagnostics challenging. 24,25,27,28,45 Similar to inhibitors that negatively impact PCR performance, RT-QuIC is susceptible to inhibitors that hamper detection and/or the misfolding of protein substrates. 7,12,15,46 Hypothesized RT-QuIC inhibitors include mucin family proteins and polar lipids^{7,46} although a variety of inhibitory factors likely exist. Traditionally, RT-QuIC inhibitors are overcome by diluting tissue samples, and concordantly reaction-limiting compounds, until diagnostic sensitivity performs as expected for true-positive samples. However, both inter- and intraindividual MP heterogeneity, as well as stage of neurodegenerative disease (i.e., early vs late stages), directly influence the quantity of MPs present within a given biological sample. Therefore, the practice of diluting diagnostic samples to overcome inhibitors may contribute to the production of false-negatives⁴⁵ (i.e., the diagnostic samples are true positives, yet have very low levels of MPs that are subsequently diluted below the limit of detection). Our data indicate that Nano-QuIC has the potential to overcome falsenegatives associated with sample dilution and/or inhibitors, as the siNP-improved assay exhibited 100% sensitivity in replicates where traditional RT-QuIC failed (Figure 5). In light of the hypothesized operational mechanism for Nano-QuIC (described above, see Figure 1C), we posit that the protein substrate (rHaPrP) binds to the siNP surface, thus increasing the local rHaPrP concentration and allowing for more efficient interaction with MPs and subsequent misfolding. This overcomes inhibitors and ultimately improves diagnostic sensitivity.

DISCUSSION

This study shows that incorporating siNPs into RT-QuIC reactions, forming Nano-QuIC, can greatly accelerate the time to detection of a prion disease (4.1 h, a 2.5× improvement). To the best of our knowledge, this is the first report of NPs being used as reagents for RT-QuIC-based diagnostics with biological samples. By analyzing kinetic data, we observed acceleration of the nucleation phase and longer growth phase time constants for reactions with SiNPs. To demonstrate the effects of other NPs, Nano-QuIC was performed with 15 nm AuNPs, an experiment that revealed AuNPs influence RT-QuIC reaction kinetics similar to siNPs. Importantly, our results indicate Nano-QuIC overcame tissue-associated inhibitor effects and significantly outperformed traditional RT-QuIC for detecting MPs at higher tissue concentrations (Figure 5a, b).

We observed that RT-QuIC reactions performed with 50 nm siNPs and a run temperature of 48 °C yielded optimal diagnostic conditions, resulting in no false positives and up to a 2.5× improvement of time to diagnosis. For this condition, the negative sample's fluorescence rise slightly due to siNPs increasing background fluorescence; however, the kinetic curves of negative control samples do not exhibit the characteristic exponential fibril growth phase, indicating that CWD-negative reactions are not seeding or creating fibril nuclei (Figure S2). The kinetic curves of diagnostic negative samples produced by Nano-QuIC are clearly distinguishable from true-positives.

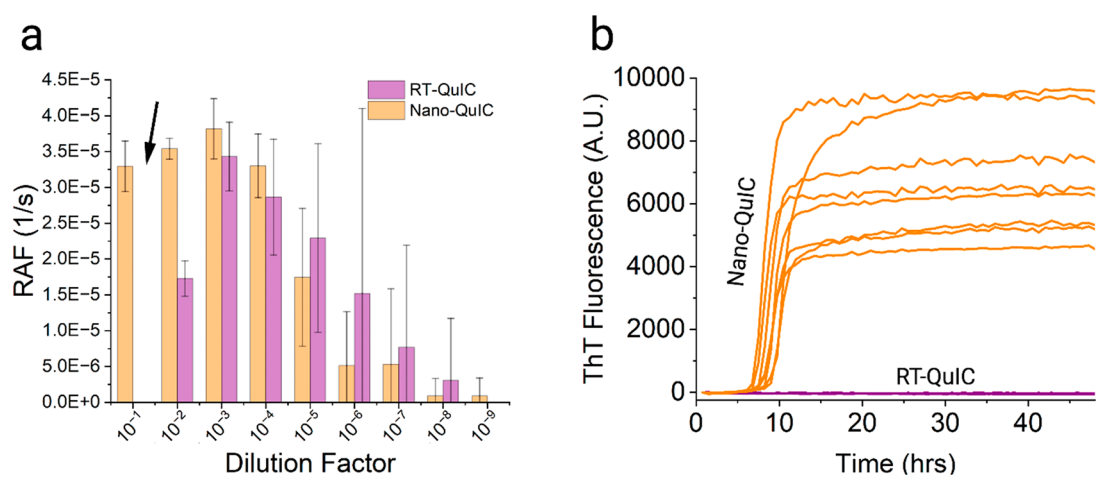


Figure 5. (a) Raw RAF for a 10-fold dilution series of CWD positive tissue amplified at 42 °C in RT-QuIC vs Nano-QuIC (50 nm siNPs, 2.5 mg/mL). Arrow highlights the lack of signal (false negative) from RT-QuIC, likely due to inhibitors. (b) Kinetic curves for 10⁻¹ CWD positive tissue dilution amplified at 42 °C in RT-QuIC versus Nano-QuIC (50 nm siNPs, 2.5 mg/mL). Unless noted otherwise, error bars show standard deviation.

Previously, NPs have been studied for their roles in promoting or preventing spontaneous amyloid formation ^{29–36} and structural impacts of amyloids. However, our work demonstrates the diagnostic potential of NPs for determining the disease status of complex biological samples, which has not been explored before. Although large, near-millimeter-scale beads have been used in RT-QuIC, ^{47–50} they did not achieve the diagnostic performance seen with siNPs in this study.

We have shown the utility of Nano-QuIC for lymph node tissue samples, which are commonly used by wildlife agencies for CWD detection. Future research on larger sample sets is needed for epidemiological validation. In addition, antemortem diagnostic applications using Nano-QuIC would be beneficial. There are a host of RT-QuIC protocols that are already developed for CWD antemortem diagnostics that likely could seamlessly incorporate nanoparticle enhancement. 51,52 Additionally, antemortem RT-QuIC protocols have been developed for a large number of noninvasive sample types across a range of human diseases such as Parkinson's, Creutzfeldt-Jakob disease (CJD), etc. 48,53,54 While different substrate proteins are used for these tests, the fundamental principle of nanoparticleaided amplification could potentially improve these assays for human disease diagnostics. Breakthroughs in traditional RT-QuIC protocols could also be readily employed in Nano-OuIC.

In conclusion, the ability of Nano-QuIC to overcome inhibitors, enhance diagnostic sensitivity and specificity, and reduce detection time collectively indicates the potential to significantly improve traditional RT-QuIC diagnostics. We note that variable results using siNPs might be observed when using protein substrates beyond the rHaPrP examined herein. It is possible that the siNP-rHaPrP interaction is specific to the protein template. Nevertheless, rHaPrP has emerged as an ideal substrate for a growing number of prion diagnostic protocols, including CJD, BSE, scrapie, and CWD. It is also possible that Nano-QuIC will require optimization for various biological and ecological samples. From a broader perspective, we believe that adaptations of Nano-QuIC will facilitate highthroughput diagnostic applications for a wide range of animal and human neurodegenerative diseases, paving the way for earlier detection and improved patient outcomes.

ASSOCIATED CONTENT

Supporting Information

The Supporting Information is available free of charge at https://pubs.acs.org/doi/10.1021/acs.nanolett.3c01001.

Methods section summarizing tissue preparation, preparation of recombinant substrate, Nano-QuIC protocols, blinded sample set, and evaluation of kinetic data (PDF)

AUTHOR INFORMATION

Corresponding Authors

Peter A. Larsen — Minnesota Center for Prion Research and Outreach (MNPRO) and Department of Veterinary and Biomedical Sciences, University of Minnesota, St. Paul, Minnesota 55108, United States; Email: plarsen@umn.edu Sang-Hyun Oh — Department of Electrical and Computer Engineering, University of Minnesota, Minneapolis, Minnesota 55455, United States; Minnesota Center for Prion Research and Outreach (MNPRO), University of Minnesota, St. Paul, Minnesota 55108, United States; orcid.org/0000-0002-6992-5007; Email: sang@umn.edu

Authors

Peter R. Christenson – Department of Electrical and Computer Engineering, University of Minnesota, Minneapolis, Minnesota 55455, United States; Minnesota Center for Prion Research and Outreach (MNPRO), University of Minnesota, St. Paul, Minnesota 55108, United States; orcid.org/0000-0003-3979-7945

Manci Li – Minnesota Center for Prion Research and Outreach (MNPRO) and Department of Veterinary and Biomedical Sciences, University of Minnesota, St. Paul, Minnesota 55108, United States

Gage Rowden – Minnesota Center for Prion Research and Outreach (MNPRO) and Department of Veterinary and Biomedical Sciences, University of Minnesota, St. Paul, Minnesota 55108, United States

Complete contact information is available at: https://pubs.acs.org/10.1021/acs.nanolett.3c01001

Nano Letters pubs.acs.org/NanoLett Letter

Author Contributions

S.-H.O. conceived the study. P.R.C. and G.R. performed molecular experiments. P.R.C., M.L., G.R., S.-H.O., and P.A.L. assisted with experimental design and interpreted the results. P.R.C., G.R., and M.L. performed statistical analyses. S.-H.O. and P.A.L. oversaw the research. All authors wrote and contributed to the final manuscript.

Funding

Funding for research performed herein was provided by the Minnesota State Legislature through the Minnesota Legislative-Citizen Commission on Minnesota Resources (LCCMR) and Minnesota Agricultural Experiment Station Rapid Agricultural Response Fund to P.R.C., M.C., G.R., P.A.L., and S.-H.O., the Sanford P. Bordeau Chair in Electrical Engineering at the University of Minnesota and the McKnight Foundation to S.-H.O., and start-up funds awarded to P.A.L. through the Minnesota Agricultural, Research, Education, Extension and Technology Transfer (AGREETT) program. Portions of this work were conducted in the Minnesota Nano Center, which is supported by the National Science Foundation (NSF) through the National Nano Coordinated Infrastructure Network (NNCI) under Award ECCS-2025124. Portions of this work were carried out in the University of Minnesota Characterization Facility, which receives partial support from the NSF through the MRSEC (Award DMR-2011401) program.

Notes

The authors declare no competing financial interest.

ACKNOWLEDGMENTS

The authors thank the staff members of the NIH Rocky Mountain Laboratories, especially Byron Caughey, Andrew Hughson, and Christina Orrù, for training and assistance with the implementation of RT-QuIC and for supplying the original rPrP clone. Jason Bartz provided helpful comments on the manuscript. M. Schwabenlander provided valuable assistance in sample acquisition. S. Stone provided valuable logistical assistance with our molecular work. F. Schendel, T. Douville, and the staff of the University of Minnesota Biotechnology Resource Center provided critical support concerning the large-scale production of recombinant proteins. K. Wilson of the Colorado State University Veterinary Diagnostic Laboratory provided assistance with ELISA and IHC testing of samples reported herein. Some figures were created using BioRender (BioRender.com).

■ REFERENCES

- (1) Prusiner, S. B. Nobel Lecture: Prions. *Proc. Natl. Acad. Sci. U.S.A.* **1998**, 95 (23), 13363–13383.
- (2) Soto, C.; Estrada, L. D. Protein Misfolding and Neuro-degeneration. Arch. Neurol. 2008, 65 (2), 184-189.
- (3) Marsh, R. F.; Kincaid, A. E.; Bessen, R. A.; Bartz, J. C. Interspecies Transmission of Chronic Wasting Disease Prions to Squirrel Monkeys (Saimiri Sciureus). *J. Virol.* **2005**, 79 (21), 13794–13796.
- (4) Kim, Y.; Park, J.-H.; Lee, H.; Nam, J.-M. How Do the Size, Charge and Shape of Nanoparticles Affect Amyloid β Aggregation on Brain Lipid Bilayer? *Sci. Rep.* **2016**, *6*, 19548.
- (5) Iranzo, A.; Fairfoul, G.; Ayudhaya, A. C. N.; Serradell, M.; Gelpi, E.; Vilaseca, I.; Sanchez-Valle, R.; Gaig, C.; Santamaria, J.; Tolosa, E.; Riha, R. L.; Green, A. J. E. Detection of α -Synuclein in CSF by RT-QuIC in Patients with Isolated Rapid-Eye-Movement Sleep Behaviour Disorder: A Longitudinal Observational Study. *Lancet Neurol* **2021**, 20 (3), 203–212.

- (6) Dong, T.-T.-T.; Satoh, K. The Latest Research on RT-QuIC Assays-A Literature Review. *Pathogens* **2021**, *10* (3), 305.
- (7) Davenport, K. A.; Hoover, C. E.; Denkers, N. D.; Mathiason, C. K.; Hoover, E. A. Modified Protein Misfolding Cyclic Amplification Overcomes Real-Time Quaking-Induced Conversion Assay Inhibitors in Deer Saliva To Detect Chronic Wasting Disease Prions. *J. Clin. Microbiol.* **2018**, *56* (9), e00947–18.
- (8) Mead, S.; Khalili-Shirazi, A.; Potter, C.; Mok, T.; Nihat, A.; Hyare, H.; Canning, S.; Schmidt, C.; Campbell, T.; Darwent, L.; Muirhead, N.; Ebsworth, N.; Hextall, P.; Wakeling, M.; Linehan, J.; Libri, V.; Williams, B.; Jaunmuktane, Z.; Brandner, S.; Rudge, P.; Collinge, J. Prion Protein Monoclonal Antibody (PRN100) Therapy for Creutzfeldt–Jakob Disease: Evaluation of a First-in-Human Treatment Programme. *Lancet Neurol* 2022, 21 (4), 342–354.
- (9) Haley, N. J.; Richt, J. A. Evolution of Diagnostic Tests for Chronic Wasting Disease, a Naturally Occurring Prion Disease of Cervids. *Pathogens* **2017**, *6* (3), 35.
- (10) Parnetti, L.; Gaetani, L.; Eusebi, P.; Paciotti, S.; Hansson, O.; El-Agnaf, O.; Mollenhauer, B.; Blennow, K.; Calabresi, P. CSF and Blood Biomarkers for Parkinson's Disease. *Lancet Neurol* **2019**, *18* (6), 573–586.
- (11) Haley, N. J.; Mathiason, C. K.; Carver, S.; Telling, G. C.; Zabel, M. D.; Hoover, E. A. Sensitivity of Protein Misfolding Cyclic Amplification versus Immunohistochemistry in Ante-Mortem Detection of Chronic Wasting Disease. *J. Gen. Virol.* **2012**, *93*, 1141–1150.
- (12) Coysh, T.; Mead, S. The Future of Seed Amplification Assays and Clinical Trials. Front. Aging Neurosci. 2022, 14, 872629.
- (13) Telling, G. C. Breakthroughs in Antemortem Diagnosis of Neurodegenerative Diseases. *Proc. Natl. Acad. Sci. U.S.A.* **2019**, *116* (46), 22894–22896.
- (14) Schwabenlander, M. D.; Rowden, G. R.; Li, M.; LaSharr, K.; Hildebrand, E. C.; Stone, S.; Seelig, D. M.; Jennelle, C. S.; Cornicelli, L.; Wolf, T. M.; et al. Comparison of Chronic Wasting Disease Detection Methods and Procedures: Implications for Free-Ranging White-Tailed Deer (Odocoileus Virginianus) Surveillance and Management. *J. Wildl. Dis.* **2022**, *58*, 50–62.
- (15) Li, M.; Schwabenlander, M. D.; Rowden, G. R.; Schefers, J. M.; Jennelle, C. S.; Carstensen, M.; Seelig, D.; Larsen, P. A. RT-QuIC Detection of CWD Prion Seeding Activity in White-Tailed Deer Muscle Tissues. *Sci. Rep.* **2021**, *11*, 16759.
- (16) Orrù, C. D.; Isiofia, O.; Hughson, A. G.; Caughey, B. Real-Time Quaking-Induced Conversion (QuIC) Assays for the Detection and Diagnosis of Human Prion Diseases. In *Prions and Diseases*; Zou, W.-Q., Gambetti, P., Eds.; Springer International Publishing: Cham, Switzerland, 2023; pp 621–635.
- (17) Nonno, R.; Di Bari, M. A.; Pirisinu, L.; D'Agostino, C.; Vanni, I.; Chiappini, B.; Marcon, S.; Riccardi, G.; Tran, L.; Vikøren, T.; Våge, J.; Madslien, K.; Mitchell, G.; Telling, G. C.; Benestad, S. L.; Agrimi, U. Studies in Bank Voles Reveal Strain Differences between Chronic Wasting Disease Prions from Norway and North America. *Proc. Natl. Acad. Sci. U.S.A.* **2020**, *117* (49), 31417–31426.
- (18) Tranulis, M. A.; Gavier-Widén, D.; Våge, J.; Nöremark, M.; Korpenfelt, S.-L.; Hautaniemi, M.; Pirisinu, L.; Nonno, R.; Benestad, S. L. Chronic Wasting Disease in Europe: New Strains on the Horizon. *Acta Vet. Scand.* **2021**, *63* (1), 48.
- (19) Otero, A.; Velásquez, C. D.; Aiken, J.; McKenzie, D. Chronic Wasting Disease: A Cervid Prion Infection Looming to Spillover. *Vet. Res.* **2021**, *52* (1), 115.
- (20) Yuan, Q.; Rowden, G.; Wolf, T. M.; Schwabenlander, M. D.; Larsen, P. A.; Bartelt-Hunt, S. L.; Bartz, J. C. Sensitive Detection of Chronic Wasting Disease Prions Recovered from Environmentally Relevant Surfaces. *Environ. Int.* **2022**, *166*, 107347.
- (21) Hannaoui, S.; Zemlyankina, I.; Chang, S. C.; Arifin, M. I.; Béringue, V.; McKenzie, D.; Schatzl, H. M.; Gilch, S. Transmission of Cervid Prions to Humanized Mice Demonstrates the Zoonotic Potential of CWD. *Acta Neuropathol* **2022**, *144* (4), 767–784.
- (22) Denkers, N. D.; Henderson, D. M.; Mathiason, C. K.; Hoover, E. A. Enhanced Prion Detection in Biological Samples by Magnetic

- Particle Extraction and Real-Time Quaking-Induced Conversion. J. Gen. Virol. 2016, 97 (8), 2023–2029.
- (23) Sepúlveda, B.; Angelomé, P. C.; Lechuga, L. M.; Liz-Marzán, L. M. LSPR-Based Nanobiosensors. *Nano Today* **2009**, *4* (3), 244–251.
- (24) Belushkin, A.; Yesilkoy, F.; Altug, H. Nanoparticle-Enhanced Plasmonic Biosensor for Digital Biomarker Detection in a Microarray. *ACS Nano* **2018**, *12* (5), 4453–4461.
- (25) Akkilic, N.; Geschwindner, S.; Höök, F. Single-Molecule Biosensors: Recent Advances and Applications. *Biosens. Bioelectron.* **2020**, *151*, 111944.
- (26) Christenson, P. R.; Li, M.; Rowden, G.; Schwabenlander, M. D.; Wolf, T. M.; Oh, S.-H.; Larsen, P. A. A Field-Deployable Diagnostic Assay for the Visual Detection of Misfolded Prions. *Sci. Rep.* **2022**, *12*, 12246.
- (27) Kumar, A.; Kim, S.; Nam, J.-M. Plasmonically Engineered Nanoprobes for Biomedical Applications. *J. Am. Chem. Soc.* **2016**, *138* (44), 14509–14525.
- (28) Jackman, J. A.; Rahim Ferhan, A.; Cho, N.-J. Nanoplasmonic Sensors for Biointerfacial Science. *Chem. Soc. Rev.* **2017**, *46* (12), 3615–3660.
- (29) Grigolato, F.; Colombo, C.; Ferrari, R.; Rezabkova, L.; Arosio, P. Mechanistic Origin of the Combined Effect of Surfaces and Mechanical Agitation on Amyloid Formation. *ACS Nano* **2017**, *11* (11), 11358–11367.
- (30) Tahaei Gilan, S. S.; Yahya Rayat, D.; Ahmed Mustafa, T.; Aziz, F. M.; Shahpasand, K.; Akhtari, K.; Salihi, A.; Abou-Zied, O. K.; Falahati, M. α-Synuclein Interaction with Zero-Valent Iron Nanoparticles Accelerates Structural Rearrangement into Amyloid-Susceptible Structure with Increased Cytotoxic Tendency. *Int. J. Nanomedicine* **2019**, *14*, 4637–4648.
- (31) Konar, M.; Mathew, A.; Dasgupta, S. Effect of Silica Nanoparticles on the Amyloid Fibrillation of Lysozyme. *ACS Omega* **2019**, *4* (1), 1015–1026.
- (32) Zhou, S.; Zhu, Y.; Yao, X.; Liu, H. Carbon Nanoparticles Inhibit the Aggregation of Prion Protein as Revealed by Experiments and Atomistic Simulations. *J. Chem. Inf. Model.* **2019**, *59* (5), 1909–1918.
- (33) Mohammadi, S.; Nikkhah, M. TiO_2 Nanoparticles as Potential Promoting Agents of Fibrillation of α -Synuclein, a Parkinson's Disease-Related Protein. *Iran. J. Biotechnol.* **2017**, *15* (2), 87–94.
- (34) Gladytz, A.; Wagner, M.; Häupl, T.; Elsner, C.; Abel, B. Structure-Making Effects of Metal Nanoparticles in Amyloid Peptide Fibrillation. *Part. Part. Syst. Charact.* **2015**, 32 (5), 573–582.
- (35) Linse, S.; Cabaleiro-Lago, C.; Xue, W.-F.; Lynch, I.; Lindman, S.; Thulin, E.; Radford, S. E.; Dawson, K. A. Nucleation of Protein Fibrillation by Nanoparticles. *Proc. Natl. Acad. Sci. U.S.A.* **2007**, *104* (21), 8691–8696.
- (36) Cabaleiro-Lago, C.; Szczepankiewicz, O.; Linse, S. The Effect of Nanoparticles on Amyloid Aggregation Depends on the Protein Stability and Intrinsic Aggregation Rate. *Langmuir* **2012**, 28 (3), 1852–1857.
- (37) Grigolato, F.; Arosio, P. The Role of Surfaces on Amyloid Formation. *Biophys. Chem.* **2021**, 270, 106533.
- (38) Zhang, D.; Neumann, O.; Wang, H.; Yuwono, V. M.; Barhoumi, A.; Perham, M.; Hartgerink, J. D.; Wittung-Stafshede, P.; Halas, N. J. Gold Nanoparticles Can Induce the Formation of Protein-Based Aggregates at Physiological pH. *Nano Lett.* **2009**, *9* (2), 666–671.
- (39) Orrú, C. D.; Hughson, A. G.; Groveman, B. R.; Campbell, K. J.; Anson, K. J.; Manca, M.; Kraus, A.; Caughey, B. Factors That Improve RT-QuIC Detection of Prion Seeding Activity. *Viruses* **2016**, *8* (5), 140.
- (40) Nielsen, L.; Khurana, R.; Coats, A.; Frokjaer, S.; Brange, J.; Vyas, S.; Uversky, V. N.; Fink, A. L. Effect of Environmental Factors on the Kinetics of Insulin Fibril Formation: Elucidation of the Molecular Mechanism. *Biochemistry* **2001**, *40* (20), 6036–6046.
- (41) Uversky, V. N.; Li, J.; Fink, Å. L. Evidence for a Partially Folded Intermediate in α -Synuclein Fibril Formation. *J. Biol. Chem.* **2001**, 276 (14), 10737–10744.

- (42) John, T.; Gladytz, A.; Kubeil, C.; Martin, L. L.; Risselada, H. J.; Abel, B. Impact of Nanoparticles on Amyloid Peptide and Protein Aggregation: A Review with a Focus on Gold Nanoparticles. *Nanoscale* **2018**, *10* (45), 20894–20913.
- (43) Alvarez, Y. D.; Fauerbach, J. A.; Pellegrotti, J. V.; Jovin, T. M.; Jares-Erijman, E. A.; Stefani, F. D. Influence of Gold Nanoparticles on the Kinetics of α -Synuclein Aggregation. *Nano Lett.* **2013**, *13* (12), 6156–6163.
- (44) Eraña, H.; Pérez-Castro, M. Á.; García-Martínez, S.; Charco, J. M.; López-Moreno, R.; Díaz-Dominguez, C. M.; Barrio, T.; González-Miranda, E.; Castilla, J. A Novel, Reliable and Highly Versatile Method to Evaluate Different Prion Decontamination Procedures. Front Bioeng Biotechnol 2020, 8, 589182.
- (45) Masson, J.-F. Surface Plasmon Resonance Clinical Biosensors for Medical Diagnostics. ACS Sens 2017, 2 (1), 16–30.
- (46) Surguchov, A. Analysis of Protein Conformational Strains-A Key for New Diagnostic Methods of Human Diseases. *Int. J. Mol. Sci.* **2020**, 21 (8), 2801.
- (47) Groveman, B. R.; Orrù, C. D.; Hughson, A. G.; Raymond, L. D.; Zanusso, G.; Ghetti, B.; Campbell, K. J.; Safar, J.; Galasko, D.; Caughey, B. Rapid and Ultra-Sensitive Quantitation of Disease-Associated α -Synuclein Seeds in Brain and Cerebrospinal Fluid by α Syn RT-QuIC. Acta Neuropathol Commun. **2018**, 6 (1), 7.
- (48) Manne, S.; Kondru, N.; Jin, H.; Serrano, G. E.; Anantharam, V.; Kanthasamy, A.; Adler, C. H.; Beach, T. G.; Kanthasamy, A. G. Blinded RT-QuIC Analysis of α -Synuclein Biomarker in Skin Tissue From Parkinson's Disease Patients. *Mov. Disord.* **2020**, 35 (12), 2230–2239
- (49) De Luca, C. M. G.; Elia, A. E.; Portaleone, S. M.; Cazzaniga, F. A.; Rossi, M.; Bistaffa, E.; De Cecco, E.; Narkiewicz, J.; Salzano, G.; Carletta, O.; et al. Efficient RT-QuIC Seeding Activity for α-Synuclein in Olfactory Mucosa Samples of Patients with Parkinson's Disease and Multiple System Atrophy. *Transl. Neurodegener.* **2019**, *8*, 24.
- (50) Fairfoul, G.; McGuire, L. I.; Pal, S.; Ironside, J. W.; Neumann, J.; Christie, S.; Joachim, C.; Esiri, M.; Evetts, S. G.; Rolinski, M.; Baig, F.; Ruffmann, C.; Wade-Martins, R.; Hu, M. T. M.; Parkkinen, L.; Green, A. J. E. Alpha-Synuclein RT-QuIC in the CSF of Patients with Alpha-Synucleinopathies. *Ann. Clin Transl Neurol* **2016**, 3 (10), 812–
- (51) Tennant, J. M.; Li, M.; Henderson, D. M.; Tyer, M. L.; Denkers, N. D.; Haley, N. J.; Mathiason, C. K.; Hoover, E. A. Shedding and Stability of CWD Prion Seeding Activity in Cervid Feces. *PLoS One* **2020**, *15* (3), No. e0227094.
- (52) Ferreira, N. C.; Charco, J. M.; Plagenz, J.; Orru, C. D.; Denkers, N. D.; Metrick, M. A., 2nd; Hughson, A. G.; Griffin, K. A.; Race, B.; Hoover, E. A.; et al. Detection of Chronic Wasting Disease in Mule and White-Tailed Deer by RT-QuIC Analysis of Outer Ear. *Sci. Rep.* **2021**, *11*, 7702.
- (53) Poggiolini, I.; Gupta, V.; Lawton, M.; Lee, S.; El-Turabi, A.; Querejeta-Coma, A.; Trenkwalder, C.; Sixel-Döring, F.; Foubert-Samier, A.; Pavy-Le Traon, A.; Plazzi, G.; Biscarini, F.; Montplaisir, J.; Gagnon, J.-F.; Postuma, R. B.; Antelmi, E.; Meissner, W. G.; Mollenhauer, B.; Ben-Shlomo, Y.; Hu, M. T.; Parkkinen, L. Diagnostic Value of Cerebrospinal Fluid Alpha-Synuclein Seed Quantification in Synucleinopathies. *Brain* **2022**, *145* (2), 584–595.
- (54) Orrů, C. D.; Groveman, B. R.; Hughson, A. G.; Zanusso, G.; Coulthart, M. B.; Caughey, B. Rapid and Sensitive RT-QuIC Detection of Human Creutzfeldt-Jakob Disease Using Cerebrospinal Fluid. *MBio* 2015, 6 (1), e02451–14.